A Correlation between Differential Structural Features and the Degree of Endopeptidase Activity of Type A Botulinum Neurotoxin in Aqueous Solution†

Shuowei Cai and Bal Ram Singh*,‡

Department of Chemistry and Biochemistry and Center for Marine Science and Technology, University of Massachusetts Dartmouth, North Dartmouth, Massachusetts 02747

Received November 3, 2000; Revised Manuscript Received February 7, 2001

ABSTRACT: Botulinum neurotoxin type A is one of the most toxic substances known to man (LD_{50} for mouse 0.1 ng/kg). It is also an effective therapeutic drug against involuntary muscle disorders and for pain management. BoNT/A is a Zn^{2+} endopeptidase which selectively cleaves SNAP-25 (synaptosomal-associated protein of 25 kDa), a critical component of the exocytotic machinery. Based on nucleotide sequence, BoNT/A is a 145 kDa protein, which appears as a 145 kDa protein band on sodium dodecyl sulfate−polyacrylamide gel electrophoresis. We have examined the structure of BoNT/A in aqueous solution, and found the structure in aqueous solution differs dramatically from that resolved by X-ray crystallography, both at secondary and at quaternary levels. In terms of secondary structure, BoNT/A in aqueous solution has about 47% β-sheet structure as revealed by infrared spectroscopy, while X-ray crystallography revealed only 17% β-sheet structure. In terms of quaternary structure, the estimated molecular mass of the native BoNT/A in aqueous solution ranged between 230 and 314 kDa, based on results from different chemical and biophysical techniques (native gel electrophoresis, chemical cross-linking, size exclusion chromatography, and fluorescence anisotropy). These results indicate that BoNT/A exists as a dimer in aqueous solution, which contrasts with the reported monomeric structure of BoNT/A based on X-ray crystallography. The dimeric form of BoNT/A can self-dissociate into the monomeric form at a concentration lower than 50 nM. This concentration-dependent structural change has a significant impact on the endopeptidase activity of BoNT/A: the catalytic efficiency of the monomeric BoNT/A is about 4-fold higher than that of its dimeric form. This difference implies a sterically restricted catalytic site of BoNT/A in the dimeric form of BoNT/A.

Clostridial neurotoxins are among the most toxic substances presently known. The LD_{50} values of clostridial neurotoxins in mouse are from 0.1 to 1 ng/kg (*1*). Two major groups of clostridial neurotoxins are botulinum neurotoxins (BoNTs)[1] and tetanus neurotoxin (TeNT), which are known to exert potent neuroparalysis effects on vertebrates, resulting in botulism and tetanus, respectively. BoNTs are classified into seven distinct serotypes, designated as A−G. Clostridial neurotoxins (BoNTs and TeNT) share a similar structural organization and mechanism of cell intoxication. Both BoNTs and TeNT are synthesized as polypetide chains of 150 kDa, which are processed by endogenous or exogenous proteases into activated dichain forms (*2, 3*). The two chains (100 kDa heavy chain and 50 kDa light chain) are linked through a disulfide bond, and consist of three functional domains (*4*): the C-terminal of the heavy chain domain (H_C) is responsible for the specific binding to synaptic terminals, the N-terminal of the heavy chain domain (H_N) is involved in the membrane translocation of the light chain or the whole toxin into the cytosol, and the light chain (LC) of clostridial neurotoxins acts as a Zn^{2+} endopeptidase (*5*). The intracellular target proteins of these toxins are critical for the docking and fusion of synaptic vesicles to the plasma membrane in the neurotransmitter release process. Unlike other Zn^{2+} endopeptidases, each BoNT serotype has highly selective target proteins and cleavage sites (*5*).

Several questions related to the molecular basis of BoNTs' action remain to be answered. How can such a big soluble protein (about 150 kDa) span a membrane and translocate a ∼50 kDa protein into the cytoplasm? How can these toxins recognize their highly specific target proteins? How can the active site of these proteins access their targets? A detailed examination of the structure−function relationship of BoNT/A is needed to answer these questions.

The recently released crystallographic structure of BoNT/A obtained under conditions where its interchain disulfide bond remains intact has revealed that BoNT/A exists as a monomer in the crystalline state (*6*). There is about 23% α-helical structure and 17% β-sheet structure in the toxin. The active site is buried about 24 Å deep in the protein matrix, making it inaccessible to its target protein, SNAP-25 (*6*). Reduction

† This work was supported by NIH Grant NS33740 and USDA Grant 95-37207-2427 to B.R.S.

* Address correspondence to this author at the Department of Chemistry and Biochemistry, University of Massachusetts Dartmouth, 285 Old Westport Rd., North Dartmouth, MA 02747. Phone: 508-999-8588. Fax: 508-999-8451. Email: bsingh@umassd.edu.

‡ A Henry Dreyfus Teacher−Scholar.

[1] Abbreviations: BoNT, botulinum neurotoxin; BoNT/A, botulinum neurotoxin type A; DTT, dithiothreitol; SDS, sodium dodecyl sulfate; PAGE, polyacrylamide gel electrophoresis; PPO, 2,5-diphenyloxazole; DTSSP, 3,3′-dithiobis(sulfosuccinimidyl propionate); 2,5-DNS-Cl, 2-dimethylaminonaphthalene-5-sulfonyl chloride; FTIR, Fourier transform infrared.

10.1021/bi0025363 CCC: $20.00 © 2001 American Chemical Society
Published on Web 03/17/2001

of the disulfide bond is believed to expose the active site (*6, 7*). The crystallographically derived β-sheet structure is dramatically different from estimates of 36% based on prediction from primary structure (*8*), or 44% based on far-UV circular dichroism (CD) analysis of BoNT/A in solution (*9*). Therefore, it is possible that there is a major difference between crystal and solution structures. The structure of BoNTs in solution has not been examined in any systematic detail, especially at the quaternary structure level. In fact, limited studies carried out so far have revealed conflicting observations (*10*). For BoNT/A, an aggregated species corresponding to trimer/tetramer was observed on native gel electrophoresis (*11, 12*). The crystalline structure of BoNT/A had initially indicated a dimeric species (*13*), but it is now believed to be a monomeric species (*6*). BoNT/A in aqueous solution was found to be a dimer as revealed by dynamic light scattering (*14*). Preliminary chemical cross-linking results have suggested the presence of both dimeric and trimeric species of BoNT/A in solution (*12*). The quaternary structures of proteins play important roles in the stabilization of native proteins (*15, 16*), and are closely related to their biological functions (*17*). The quaternary structure derived from X-ray crystallography, however, is not reliable, because under crystallization conditions the quaternary structure may change (*18, 19*). The secondary structure resolved from X-ray crystallography is different from the solution structure in certain other proteins also (*19*). A clear understanding of the structure of BoNTs in solution is essential, not only because of conflicting reports but also because it could hold the key to the understanding of the molecular basis of unique Zn^{2+} endopeptidase activity, as well as translocation of the neurotoxin across the neuronal membrane. A major unique feature of BoNT endopeptidase activity is the requirement of its disulfide bond reduction for activation (*7, 20*−*23*). Very little, if any, information is currently available on the structure of BoNT/A under conditions where its disulfide bond is reduced (enzymatically active form).

The low LD_{50} of BoNTs indicates that an extremely low concentration of BoNT is active under physiological conditions (10^{-15}−10^{-16} M range in the animal body fluids) (*24*). It is estimated that once the toxin gets into the neuronal cytosol, a single molecule of enzymatic active toxin is sufficient to intoxicate a synapse (*25*). The effective concentration for BoNT/A to block neurotransmitter release on a nueromuscular junction has been determined as 10^{-8}−10^{-9} M (*27*). An understanding of BoNT's structure in solution at physiological concentration is therefore essential to provide a detailed mechanism involved in its action. However, all structural information about BoNTs so far is based on relatively high protein concentration.

In our current study, we, for the first time, have systematically investigated the structure of BoNT/A in solution state using different biophysical techniques. We also describe the quaternary structure of BoNT/A at a concentration lower than 5 nM, using fluorescence anisotropy. Our results suggest that BoNT/A has about 31% α-helical structure, 47% β-sheet, 15% random coil, and 6% β-turns under nonreducing conditions, as revealed by Fourier transform infrared (FTIR) spectroscopy. Under reducing conditions, the secondary structure does not change very much. However, the tertiary structure becomes more flexible. BoNT/A exists as a dimer in solution. The dimeric form of BoNT/A self-dissociates into the monomeric form at concentrations below 50 nM. Examination of the endopeptidase activity of dimeric and monomeric forms of BoNT/A under reducing conditions, by measuring the cleavage of its intracellular target protein, SNAP-25, revealed that the enzymatic activity of the monomeric form is about 4-fold higher than that of its dimeric form.

MATERIALS AND METHODS

Botulinum Neurotoxin Preparation. Botulinum neurotoxin type A was purified from the cultures of *C. botulinum* strain Hall according to the methods described previously (*27*). The purity of BoNT/A was checked with sodium dodecyl sulfate (SDS)−polyacrylamide gel electrophoresis. Pure BoNT/A showed only one single band at approximately 145 kDa on a 12% SDS−polyacrylamide gel under nonreducing conditions. Pure toxin sample was then dialyzed against 20 mM sodium phosphate buffer, pH 7.2. The reduced toxin was prepared by treating it with 20 mM dithiothreitol (DTT) for 30 min at 37 °C. To remove the excess DTT, the sample was then dialyzed against 20 mM sodium phosphate buffer, pH 7.2, containing 1 mM DTT. The concentration of BoNT/A was determined by using the published extinction coefficient at 280 nm (*27*).

FTIR Spectroscopy of BoNT/A. FTIR spectra of BoNT/A were collected using a Nicolet 8210 FTIR spectrometer, equipped with a zinc selenide attenuated total reflectance (ATR) accessory and DTGS detector. The resolution was set at 4 cm^{-1}, and each recorded spectrum was the average of 256 scans.

Native Gel Electrophoresis. The Tris−glycine buffer system was chosen for native gel electrophoresis (*28*). The electrophoresis was run using a Hoefer SE 250 Mighty Small II Mini-Gel System from Amersham Pharmacia Biotech (Piscataway, NJ). The electrophoresis was run under a constant voltage of 200 V at room temperature, except for the time-dependent experiment. For the time-dependent experiment, the electrophoresis was run under a constant voltage of 200 V at 4 °C. Two methods have been developed to calibrate the native gel electrophoresis results. In one method, Ferguson plots are generated by electrophoresing the given protein as well as standard proteins on a set of homogeneous polyacrylamide gels with different polyacrylamide concentrations (*28, 29*), and by determining the relative protein mobility in terms of R_f values for each gel. The plot of 100 log ($100R_f$) against the percent gel concentration is called the Ferguson plot. The slope of the Ferguson plot is called the retardation coefficient (K_R), which is only dependent on the protein size. To perform the Ferguson plot, polyacrylamide homogeneous gels of different concentrations (6%, 6.5%, 7%, 7.5%, and 8%) were cast. The high molecular mass native protein calibration kit (thyroglobulin, 669 kDa; ferritin, 440 kDa; catalase, 232 kDa; lactate dehydrogenase, 140 kDa; albumin, 67 kDa) (Amersham Pharmacia Biotech, Piscataway, NJ) was used for molecular mass standards. The plot of retardation coefficient vs molecular mass standards was used to estimate the molecular size of BoNT/A.

In another method, protein size is determined from the native gel electrophoresis experiment by using a linear gradient polyacrylamide gel. The pore radius of the gradient

gel increases with decreasing gel concentration (*30*). When proteins reach their pore limit in a gradient gel, their migration rate approaches zero. The migration distance (D) of the protein at its pore limit is called the maximum migration distance (D_{max}). At this point, the influence of charge on the final migration position of a protein is eliminated so that D_{max} is the function only of protein size and shape. Of course, the time required for a given protein to reach its pore limit is usually long, and is still dependent on its charge. By running samples at different time points on the linear gradient gel and plotting the transformed migration values [ln (ln (D)] vs the reciprocal of square roots of times of electrophoresis ($t^{-1/2}$), the D_{max} can be obtained from the intercept on the plot. To perform time-dependent linear gradient gel electrophoresis, a 5−20% linear gradient gel was cast. To calibrate the molecular mass of BoNT/A, the gel was run for different periods of time (1.5, 2, 4, 6, 12, and 15 h). The molecular mass standards used in the linear gradient gel were the same as the ones used for homogeneous gels. Ten micrograms of protein was loaded in each lane in both cases.

Size Exclusion Chromatography. Chromatograms were collected using a Waters 515 HPLC system equipped with a dual-wavelength absorbance detector (Waters, Milford, MA). The HPLC system was operated by Millennium^{32} software. A Protein Pak 300 column [7.5 mm (i.d.) × 30 cm] (Waters) was used to calibrate the molecular mass of BoNT/A. Peaks were monitored at 214 nm. The column was preequilibrated with 20 mM sodium phosphate buffer, pH 7.2. Apoferritin (443 kDa), γ-globulin (158 kDa), ovalbumin (44 kDa), and myoglobin (17 kDa) (Bio-Rad Laboratories, Hercules, CA) were used as gel filtration protein standards to calibrate the column for molecular weight estimations. A 20 μL sample was injected into the column each time. The concentration of the toxin injected was 1.5 mg/mL. The elution rate was fixed at 0.7 mL/min with a constant pressure of 325 psi.

Chemical Cross-Linking of BoNT/A. 3,3′-Dithiobis(sulfosuccinimidyl propionate) (DTSSP) (Pierce, Rockford, IL) was used to cross-link BoNT/A. DTSSP is a water-soluble cross-linker with an 11 Å spacer, which is reactive toward primary amines on the side chains of amino acids such as lysine residues. Three micromolar BoNT/A in 20 mM sodium phosphate buffer, pH 7.2, was incubated with 100 μM DTSSP (final concentration) at room temperature (25 °C) for 10 min. The reaction was stopped by adding 1 M Tris, pH 7.5, to a final concentration of 25 mM in the reaction mixture. The cross-linking reaction products were analyzed by 4% SDS−polyacylamide gel electrophoresis under nonreducing conditions.

Preparation of 2,5-DNS-Cl-Labeled Toxin. One milligram of 2-dimethylaminonaphthalene-5-sulfonyl chloride (2,5-DNS-Cl) (Molecular Probes, Eugene, OR) was dissolved in 100 μL of anhydrous dimethylformamide (DMF) (Sigma Chemical Co., St. Louis, MO). Then 50 μL of DNS-Cl solution was slowly added into about 1 mL of 1.5 mg/mL toxin solution in 20 mM sodium phosphate buffer, pH 7.2. The reaction was allowed to proceed for 1 h at 4 °C, with continuous stirring. The reaction was stopped by adding 0.1 mL of freshly prepared 1.5 M hydroxylamine. The labeled toxin was then purified through a Sephadex G-25 column (Sigma Chemical Co.). The dye-to-protein ratio was determined by using the method provided by Molecular Probes (*31*).

Fluorescence Anisotropy Measurements. The fluorescence lifetime of 2,5-DNS-labeled protein was derived from measurements of the modulation frequency response of 2,5-DNS to excitation at 360 nm, with fluorescence emission recorded through a 54.7° polarizer and a 420 nm cutoff filter. Measurements of the demodulation and phase angle of fluorescence were made relative to those of 2,5-diphenyloxazole (PPO, Sigma Chemical Co.) in ethanol, using a lifetime of 1.40 ns. Data were collected in the frequency domain using an ISS K2 Multifrequency Phase Fluorometer (Champaign, IL). The anisotropy of 2,5-DNS-labeled protein was measured using the same fluorometer under steady-state conditions. The measurement was carried out in the L-format, exciting with 360 nm polarized light and measuring the emission through the 420 nm cutoff filter.

The limiting anisotropy and rotational correlation time of DNS-labeled toxin samples for their molecular weight estimations were calculated according to the methods described by Lakowicz (*32*):

$$1/r = 1/r_0(1 + \pi/\phi) = 1/r_0(1 + \pi RT/V\eta)$$

where r is the measured anisotropy, r_0 is the limiting anisotropy measured in the absence of rotational diffusion, ϕ is the rotational correlation time for the diffusion process, π is the lifetime of the fluorophore, R is the gas constant, T is the temperature in degrees Kelvin, η is the viscosity of the solution, and V is the molecular volume of the fluorophore. By plotting $1/r$ vs T/η (Perrin plot), both limiting anisotropy and molecular volume of the fluorophore can be obtained. The molecular volume can then be related to the molecular weight, M, of the fluorophore by the equation:

$$\phi = V\eta/RT = (V_h + h)(M\eta)/RT$$

where V_h is the specific volume of the protein, which is near 0.73 mL/g, and h is the hydration, typically 0.2 g of H_2O/g of protein.

To get the isothermal Perrin plot, we varied the viscosity by adding sucrose in the solution, while keeping the temperature constant.

To examine the self-dissociation of BoNT/A, the steady-state fluorescence anisotropy of 2,5-DNS-labeled protein was measured at room temperature (25 °C) as a function of protein concentration of BoNT/A by sequential dilution with 20 mM phosphate buffer, pH 7.2. As a control experiment, we diluted 2,5-DNS-labeled toxin with unlabeled toxin. This allowed us to evaluate the possibility of a decrease in anisotropy due to a decrease of the fluorescence signal upon dilution.

Tryptophan Anisotropy Spectra. The anisotropy spectra were collected using the same fluorometer under steady state. The measurement was carried out in the L format, with excitation with 295 nm polarized light and emission monitored through the monochromator and polarizer. The resolution of the emission monochromotor was set up at 1 nm.

Endopeptidase Activity Assay. To obtain the enzyme kinetic parameters of BoNT/A, the desired concentrations of GST−SNAP-25 fusion protein were incubated with either 20 nM or 200 nM reduced or nonreduced toxin at 37 °C.

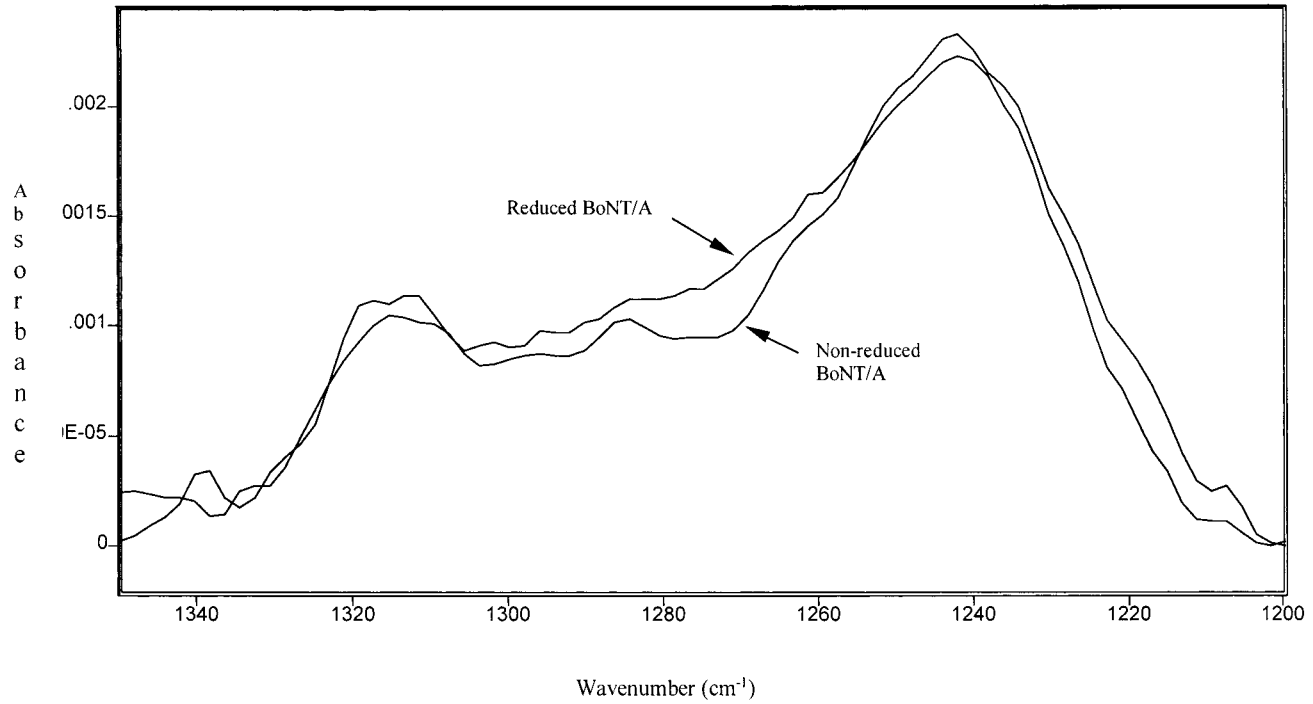

FIGURE 1: Amide III region of FTIR spectra of reduced and nonreduced BoNT/A. IR spectra of native or reduced (reduced toxin was prepared as described under Materials and Methods) BonT/A (0.34 mg/mL) dissolved in 20 mM NaBP buffer, pH 7.2, were collected at room temperature (25 °C). A reference spectrum corresponding to the buffer was recorded under identical conditions. The protein spectra were obtained by subtraction of the buffer spectra according to the reported criteria (*33*).

The initial velocity of the reaction was determined through the first 5 min reaction. The reaction was then stopped by adding trifluoroacetic acid (TFA) to a final concentration of 0.1%. The samples were then analyzed by reverse-phase HPLC using a Waters 515 HPLC system equipped with a dual-wavelength absorbance detector (Waters Corp., Milford, MA) and a Symmetry 300 C_{18} column (4.6 × 250 mm, 5 μm particle size, 300 Å pore size; Waters). To prepare reduced toxin samples, different concentrations of toxin were pretreated with 20 mM dithiothreitol (DTT) for 30 min at 37 °C.

The sample was eluted using a linear gradient from 0% eluent A to 30% eluent B in 30 min, and 30% eluent B/70% eluent A to 100% eluent B in 15 min, where eluent A was 0.1% TFA/water (v/v) and eluent B was acetonitrile/water (70:30) + 0.085% TFA (v/v).

The cleavage product was quantified using the synthesized nine amino acid peptide corresponding to the cleavage product of SNAP-25 (RATKMLGSG) (New England Peptide, Fitchburg, MA) as a standard.

RESULTS

Secondary Structure of BoNT/A in Solution. The secondary structure of BoNT/A in solution was monitored by FTIR spectroscopy. The IR spectra were resolved by using the curve-fitting program (Galactic Industry Corp., Salem, NH). The amide III spectral region of protein was used to analyze protein secondary structure (*33*). Under nonreducing conditions, BoNT/A has about 31% α-helix, 47% β-sheet, 6% β-turn, and 15% random coil in aqueous solution. Under reducing conditions, the secondary structure of BoNT/A did not show any significant change (Figure 1).

Tertiary Structure of BoNT/A under Reducing and Nonreducing Conditions. The tertiary structure of BoNT/A shows a significant change under reducing conditions revealed by tryptophan anisotropy spectra (Figure 2). The decreased anisotropy of tryptophan indicated that the tryptophan topography in the protein becomes more flexible. The red shift of the maximum anisotropy from 324 nm under nonreducing conditions to 333 nm under reducing conditions reflected that tryptophan residues of BoNT/A under reducing conditions are more exposed to the solvent. This finding is consistent with our earlier observation (*7*) that the reduced toxin adopted a more flexible structure.

Quaternary Structure of BoNT/A in Solution. The quaternary structure of BoNT/A in solution was monitored by native gel electrophoresis, chemical cross-linking reaction, fluorescence anisotropy, and size exclusion chromatography. The estimated molecular sizes of BoNT/A from different biochemical and biophysical techniques are summarized in Table 1.

Native polyacrylamide gel electrophoresis is a widely used method to estimate the molecular size of native proteins (*28*, *34*). Unlike SDS−polyacrylamide gel electrophoresis, the migration distance of protein on the native polyacrylamide gel is dependent on the molecular size and surface charge of the protein. Therefore, estimation of molecular size from native gel electrophoresis should be carried out cautiously by choosing suitable calibration methods to remove charge interference.

In this study, we used two methods to calibrate the molecular size of BoNT/A in solution, as described under Materials and Methods. The native gel clearly showed two bands for BoNT/A. A major band appeared at high molecular size position with shorter distance of migration, and a second minor band appeared at low molecular size position with longer distance of migration (Figure 3). By using Ferguson plot analysis (Figure 4, A and B), we estimated the molecular

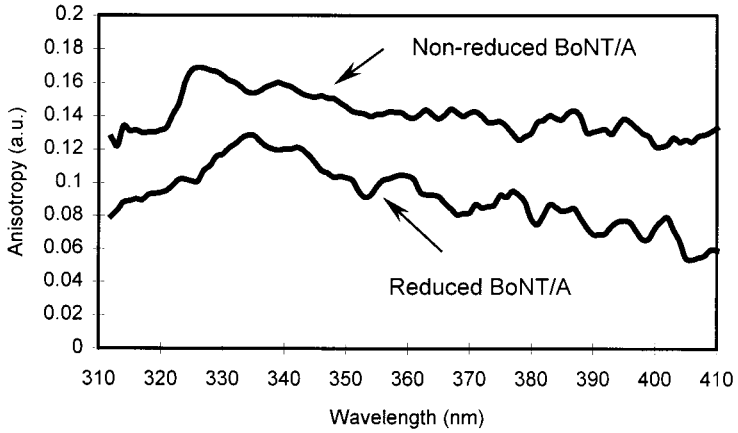

FIGURE 2: Anisotropy spectra of reduced and nonreduced BoNT/A. The protein was excited at 295 nm. Each spectrum is the average of 5 scans and is smoothed by using a 3-point window.

Table 1: Summary of Molecular Mass of Native BoNT/A in Solution Estimated from Different Biochemical and Biophysical Techniques under High Concentration (above 200 nM)

techniques	molecular mass (kDa)
native PAGE	
Ferguson plot	270 (major band), 142 (minor band)
time-dependent gradient PAGE	245 (major band), 136 (minor band)
size exclusion chromatography	453 (aggregation peak), 230 (major peak), 105 (anomalous peak, see text)
chemical cross-linking	314
fluorescence anisotropy	286

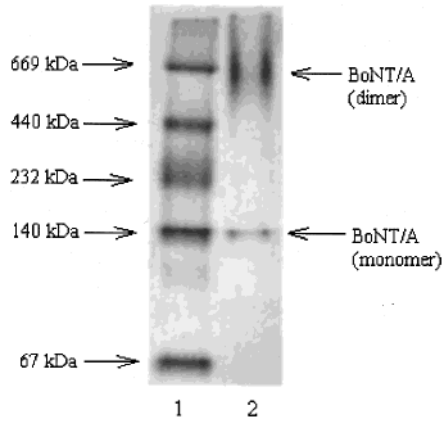

FIGURE 3: Native gel electrophoresis of BoNT/A on a 7% polyacrylamide gel showing two bands of BoNT/A (lane 2). Lane 1 is the molecular mass standards.

mass of the major band to be approximately 270 kDa, and that of the minor band as about 142 kDa. The molecular masses of the major and minor bands of BoNT/A from time-dependent gradient native gel electrophoresis were estimated to be 245 and 136 kDa, respectively (Figure 4, panels C and D). The results from native gel electrophoresis clearly showed that BoNT/A existed as two molecular species in solution. The major species is a dimeric form, and the minor species is a monomeric form of BoNT/A. These results are consistent with our earlier preliminary observations (*12*).

Size exclusion chromatography of BoNT/A showed three elution peaks (Figure 5) corresponding to molecular masses of 453, 230, and 105 kDa, respectively. The first peak arises apparently from an aggregation species of BoNT/A, and the second peak is likely from the dimeric form of BoNT/A. The third peak is anomalous, as its molecular size calibrated from the molecular standard is much lower than the monomeric form of BoNT/A, and the peak exhibits a strong tailing profile. This indicates that the protein has significant interaction with the matrix of the column. The protein−matrix interaction is common in size exclusion chromatography (*35*). Therefore, we suspect that the third peak in the size exclusion chromatogram (Figure 5) results from the protein−matrix interactions.

Chemical cross-linking is a widely used method to study protein quaternary structure (*36*). Here, we used DTSSP as a cross-linker to study the quaternary structure of BoNT/A. Cross-linked product was analyzed by SDS−polyacrylamide gel electrophoresis. The intensity of the monomeric form of BoNT/A, corresponding to a molecular mass of 135 kDa as calculated from the two-point calibration curve of 116 and 220 kDa protein standards, significantly decreased after cross-linking. The decrease was accompanied with a concomitant appearance of the dimer form of BoNT/A, corresponding to a molecular mass of 314 kDa (Figure 6, lane 3). A faint band of 507 kDa, which appeared to be a trimeric species, and some aggregated oligomeric species, located on the top of the stacking gel, were also observed in lane 3 of Figure 6. The trimeric and other oligomeric forms of BoNT/A might arise from nonspecifically aggregated protein molecules, because the protein concentration used in cross-linking experiment was relatively high (*37*). It is worth noting that the amount of dimer was small compared to the amount of residual monomer. This is believed to be the consequence of nonspecific intramolecular derivatization during the cross-linking process, causing a rapid dissociation of the dimer in the presence of SDS (*37*). To evaluate the specific nature of the oligomeric species of BoNT/A, we treated the sample with different concentrations of urea before the cross-linking reaction. In general, when sample was treated with urea before the cross-linking reaction, it was apparent that the monomer form of BoNT/A increased in low concentration urea solutions (<5 M) (Figure 6, lanes 4−7), while in high concentration urea solutions (>6 M), BoNT/A was completely aggregated (Figure 6, lanes 8−10). This indicated that low concentrations of urea dissociated the dimer form of BoNT/A, while high concentrations of urea denatured the protein, and caused formation of intramolecular aggregates (*38*). Importantly, at least some dimeric species were observed even after treatment with up to 5 M urea (Figure

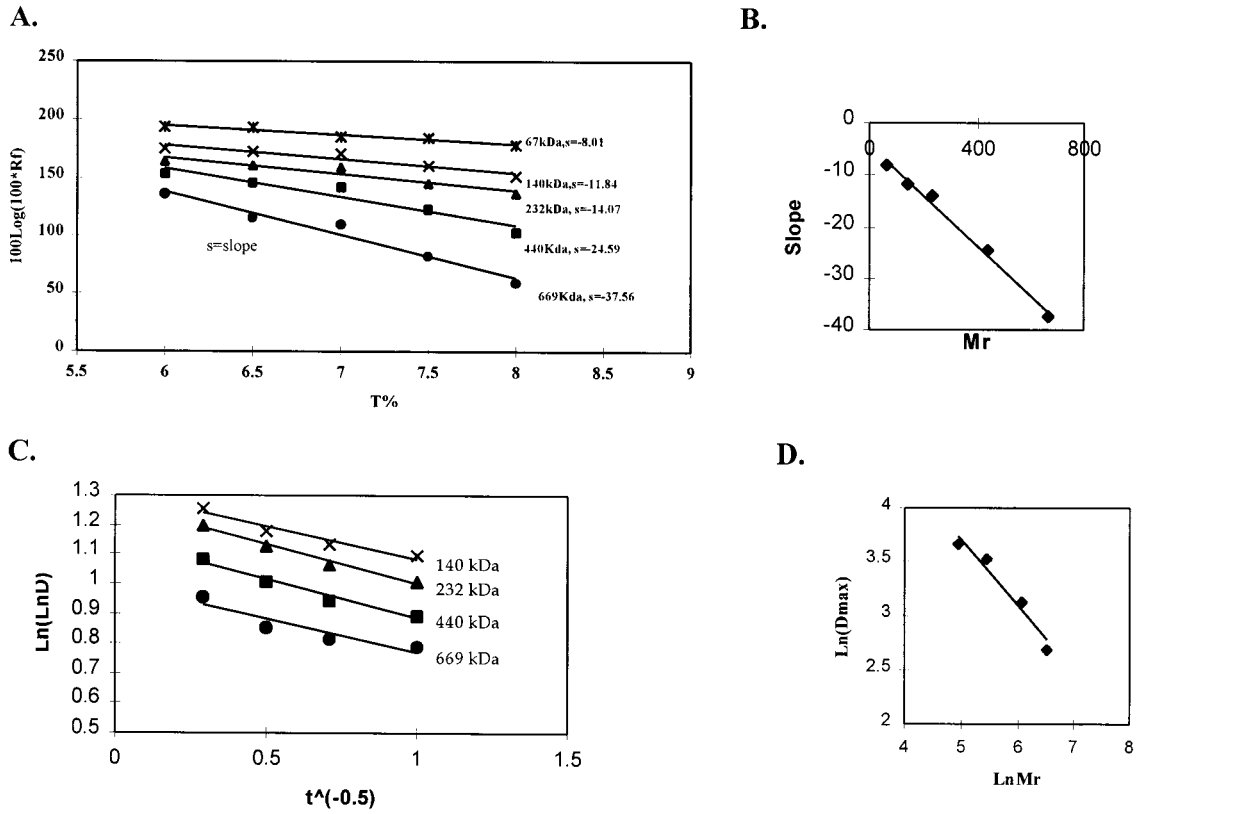

FIGURE 4: Calibration curves of the Ferguson plot and time-dependent gradient gel electrophoresis. Panels A and B show the Ferguson plot of 5 protein standards (67, 140, 232, 440, and 669 kDa), and their resultant respective calibration curves. Panel C shows the plot of ln (ln *D*) vs reciprocal of square root of the time of electrophoresis for the four standards (140, 232, 440, and 669 kDa) on a 5−20% gradient gel. Panel D shows the calibration curve of ln M_r vs ln D_{max} for time-dependent gradient native gel electrophoresis.

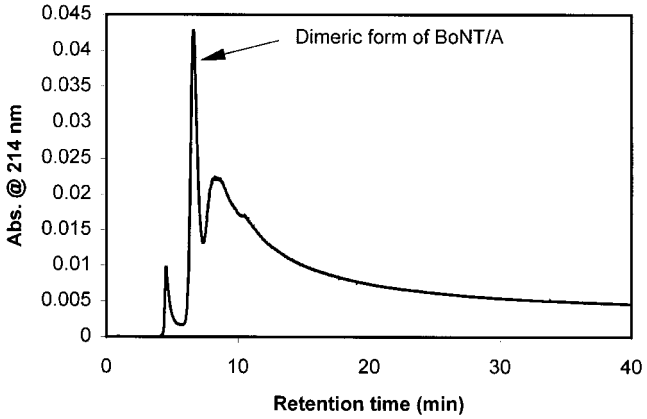

FIGURE 5: Gel filtration chromatogram of nonreduced BoNT/A. The concentration of BoNT/A was 1 mg/mL. 20 μL was loaded onto the Protein Pak 300 column (7.5 × 300 mm) (Waters, Milford, MA). The peak was monitored at an absorbance of 214 nm. Gel filtration standards from Bio-Rad (434, 158, 44, and 17 kDa) were used to calibrate the molecular mass of BoNT/A.

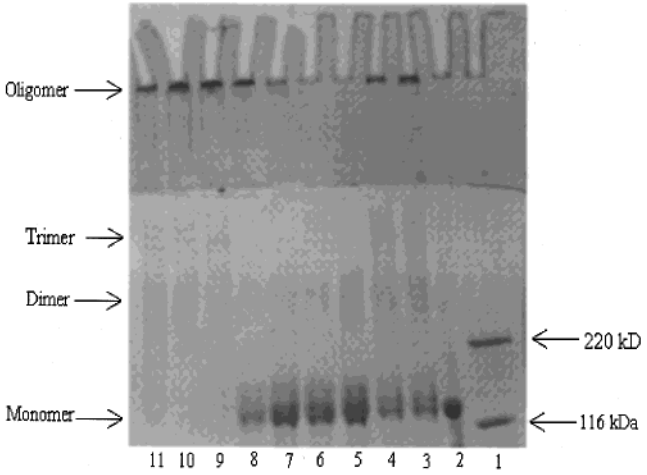

FIGURE 6: SDS−PAGE analysis of chemical cross-linking products of BoNT/A, with DTSSP as the cross-linker. Lane 1, molecular mass standards; lane 2, BoNT/A without cross-linking, and in the absence of urea; lane 3, BoNT/A cross-linked through DTSSP in the absence of urea; lanes 4−11, BoNT/A cross-linked through DTSSP in the presence of different concentrations of urea (1−8 M, respectively).

6, lane 7), indicating a specific (strong) nature of the association between BoNT/A molecules. Weak interactions among BoNT/A molecules also seem to exist, resulting in trimers, which dissociate at urea concentrations higher than 2 M (Figure 6, lane 5).

We further used fluorescence to probe the quaternary structure of BoNT/A in solution. During excitation with polarized light, one selectively excites those fluorophore molecules whose absorption transition dipole is parallel to the electric vector of the excitation light. This selective excitation results in partial fluorescence emission called polarization or anisotropy. Several phenomena can decrease the measured anisotropy to values lower than the maximum possible values. This is called fluorescence depolarization. The most common reason for depolarization is the rotational diffusion of molecules. The correlation time for the diffusion process can be measured from the fluorescence depolarization, and this correlation time is related to the molecular size of the fluorophore, and therefore is used to probe protein sizes.

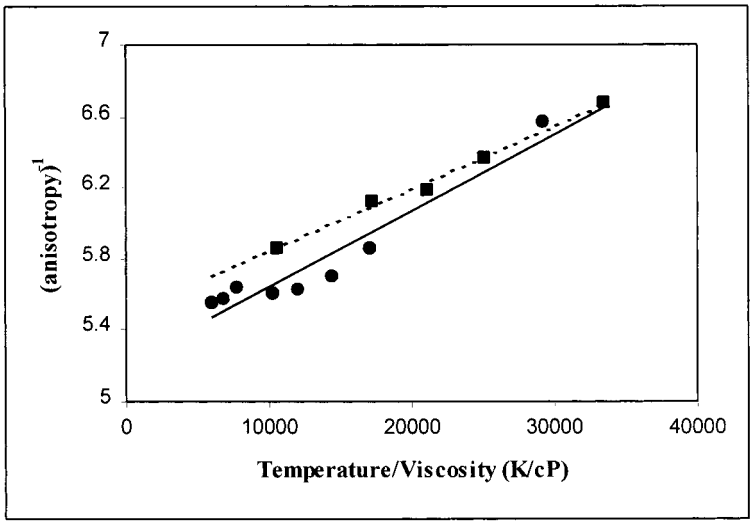

FIGURE 7: Perrin plots of dansylated toxin under native and reduced conditions. The solid line with circles represents 200 nM BoNT/A under native conditions; the dashed line with squares represents 200 nM BoNT/A under reducing conditions. Viscosity of samples was varied isothermally (at 25 °C) by the inclusion of sucrose.

Table 2: Fluorescence Lifetime, Rotational Correlation Time of 2,5-DNS-Labeled BoNT/A, and Estimated Molecular Mass of BoNT/A under Native and Reducing Conditions

BoNT/A	concn (nM)	π (ns)	ϕ (ns)	molecular mass (kDa)
native state	200	25.7	97	286
	20	28.2	54	160
reduced state	200	27.8	85	245
	20	26.2	43	130

The internal tryptophan residues in the protein are generally not suitable to study the molecular size of large proteins by using fluorescence depolarization because of relatively short fluorescence lifetimes. An external fluorescence probe with longer lifetime would be desired to study protein size. Here we chose 2,5-DNS-Cl as an external fluorescence probe, because it has a long fluorescence lifetime (about 30 ns) and, therefore, is suitable to study large proteins (*39*) such as BoNT/A.

After labeling BoNT/A with 2,5-DNS-Cl, the molar ratio of 2,5-DNS to BoNT/A in the dansylated toxin was determined to be about 1. This means only one 2,5-DNS molecule was attached on one toxin molecule. The CD spectra of DNS-labeled protein showed that there is no significant change in the structure of BoNT/A due to probe attachment (data not shown).

To obtain the size information of dansylated toxin, we calculated the limiting anisotropy and rotational correlation time from the Perrin plot (*32*). Figure 7 shows the Perrin plots for BoNT/A under native and reduced conditions. The rotational correlation times, fluorescence lifetimes, and molecular masses calibrated from correlation times of BoNT/A under different conditions (native and reducing) are summarized in Table 2. The molecular mass estimated from fluorescence depolarization clearly showed that at a concentration of 200 nM, BoNT/A exists in a dimeric form (molecular mass about 286 kDa).

One of the unique characteristics of BoNT/A is that the reduction of the disulfide bond between heavy and light chains is essential for its endopeptidase activity (*20*−*23*). Therefore, we further analyzed the molecular size of toxin under reduced conditions (Table 2). The results were similar to those under nonreduced conditions, except that the molecular mass was smaller (245 kDa). It is known that reduction of the disulfide bond in BoNT/A leads to a more flexible structure (*7*). The smaller molecular mass may reflect the fact that the protein shape changes due to a more flexible state under reducing conditions and, therefore, BoNT/A molecules tumble faster (*32*).

Self-Dissociation of the Dimeric Form of BoNT/A to the Monomeric Form. Steady-state fluorescence anisotropy of dansylated BoNT/A was measured as a function of its concentration. The concentration-dependent anisotropy curve (Figure 8) showed a dramatic decrease between 75 and 50 nM BoNT/A, suggesting a concentration-dependent transition in the molecular size. Dilution of an oligomeric protein sample to an appropriate concentration range results in a shift of the equilibrium of subunit interaction toward the dissociated species due to mass action. Since the size of the dissociated form of the oligomer is smaller than its associated form, it tumbles faster in solution. This decrease in the correlation (or tumbling) time leads to an overall decrease in the measured fluorescence anisotropy. Therefore, any protein concentration-dependent anisotropy change is necessarily the result of a shift in the protein subunit association equilibrium. As a control experiment, we diluted dansylated BoNT/A with unlabeled BoNT/A. The anisotropy of dansylated protein remained the same upon dilution with unlabeled BoNT/A, indicating that the BoNT/A still remained in a dimeric form. The above observation suggests that the decrease in anisotropy of dansylated toxin is the result of dissociation of the dimeric form of the toxin, and not due to any error from the fluorescence signal decrease with the dilution.

To investigate effects of concentration of toxin on its quaternary structure, we examined the molecular mass of dansylated toxin at low concentration (20 nM) using fluorescence depolarization. The summary of molecular mass of BoNT/A at low concentration is also listed in Table 2. The molecular mass (about 286 kDa) calibrated from fluorescence depolarization clearly indicated that at high concentration BoNT/A existed in a dimeric form, while at low concentration it existed in a monomeric form (molecular

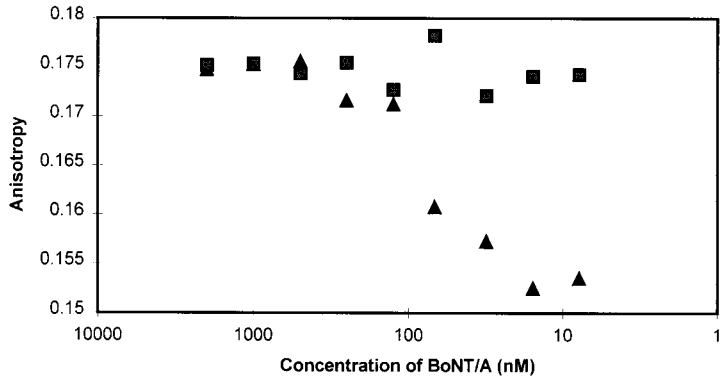

FIGURE 8: Dilution profiles of steady-state anisotropy of 2,5-DNS-labeled toxin with buffer (triangles) and nonlabeled toxin (squares) as described under Materials and Methods.

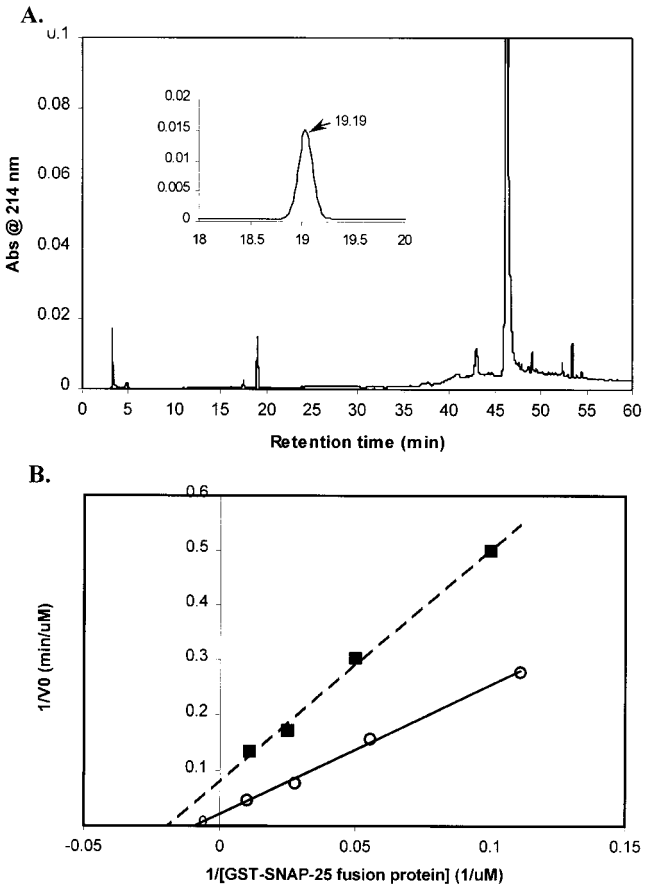

FIGURE 9: (A) Chromatographic analysis of the cleavage of GST−SNAP-25 fusion protein (20 μM) by 200 nM reduced BoNT/A. The mixture was incubated at 37 °C for 2 h. The reaction was stopped by adding TFA to a final concentration of 0.1%. The sample was eluted with a linear acetonitrile/0.085% TFA gradient, as described under Mateirals and Methods. The inset panel is the expansion of the region of retention times 18−20 min, showing the peptide peak appearing upon incubation with BoNT/A (retention time of 19.19 min). This peak does not overlap with any of the peaks present in the buffer-treated GST−SNAP-25 fusion protein. (B) Lineweaver−Burk plots of cleavage of GST−SNAP-25 fusion protein by 200 nM reduced BoNT/A (circles) or 20 nM reduced BoNT/A (squares). A series of GST−SNAP-25 concentrations (100, 40, 20, and 10 μM) were used.

mass about 160 kDa). In view of the existence of the dimeric and monomeric molecular species of BoNT/A at high and low concentrations, the concentration-dependent transition in the fluorescence anisotropy observed at 50−75 nM represents an equilibrium between these two structural forms.

Table 3: Enzyme Kinetic Parameters of Dimeric and Monomeric Forms of BoNT/A under Reducing Conditions

enzyme	K_m (μM)	k_{cat} (min^{-1})	k_{cat}/K_m (μM^{-1} min^{-1})
dimeric form	106 ± 12	251 ± 32	2.3
monomeric form	51 ± 15	603 ± 68	12

Enzymatic Activity Difference between the Two Structural Forms of BoNT/A. Difference in the biological activity of BoNT/A in its different structural states can help resolve its molecular mechanism of action, which is important to BoNT's clinical application, and for developing antidotes against botulinum. Since the existence of monomeric and dimeric forms of BoNT/A in aqueous solution depends on its concentration, it became readily possible to test any differences in the biological activity of the two types of BoNT/A structure.

The biological activity of BoNT/A is directly related to its endopeptidase activity (*22*, *23*). Therefore, we used BoNT/A's intracellular target protein, synaptosome-associated protein of 25 kDa (SNAP-25), as the substrate to evaluate endopeptidase activities of the two structural forms of BoNT/A. BoNT/A cleaves the C-terminal of SNAP-25, between Q^{197} and R^{198}, truncating nine amino acids (*40*). We used reverse-phase HPLC to monitor the cleavage product (Figure 9A). SNAP-25 used in our experiments was expressed as SNAP-25−glutathione *S*-transferase (GST−SNAP-25) fusion protein in *Escherichia coli* DH1αF′ strain (*7*). We investigated the enzymatic behavior of dimeric and monomeric forms of BoNT/A under conditions when the disulfide bond between the two chains of BoNT/A was reduced. Enzyme kinetic parameters of the two structural forms of BoNT/A (Table 3) demonstrate that the kinetic behavior of the reduced BoNT/A is concentration-dependent, and the monomeric form of BoNT/A has about 4-fold higher catalytic efficiency than the dimeric form of BoNT/A.

To accurately compare the enzyme kinetic parameters of the two structural forms of BoNT/A observed at two different concentrations, the enzyme concentration must be optimized before performing the enzyme kinetic assay. The enzyme concentration used for estimating kinetic parameters should be within the range which shows a linear relationship with the initial velocity of the reaction. Therefore, we examined the linear concentration range for both dimeric and monomeric forms of BoNT/A. The linear concentration range for the dimeric form of BoNT/A was 0−250 nM (0, 100, 150, 200, and 250 nM), whereas for the monomeric form it was

0−30 nM (0, 10, 15, 20, 30 nM) (data not shown). However, the slopes were different, indicating that their enzymatic behaviors are different.

DISCUSSION

BoNT/A is the most toxic substance known to man. However, the molecular mechanism of its action is still not clear. To fully understand the mechanism of action of BoNT/A, it is necessary to examine its structure. In this paper, we, for the first time, systematically analyze the structure of BoNT/A in solution at secondary, tertiary, and quaternary levels, using an array of biophysical methods. We chose several techniques to estimate the molecular size of BoNT/A, because all the methods we used in this paper are low-resolution methods compared to X-ray crystallography. By using different methods, we can overcome the limitations of each individual method, and get a comprehensive picture of the structural information of BoNT/A in solution.

The secondary structure analyzed from IR spectra suggests that the β-sheet content of BoNT/A is about 47%, which is different from the X-ray crystallographic estimate of about 17% β-sheet content in the protein. Our estimates are close to the computer prediction employing the neural network program (*8*). The difference indicates that the structural organization is different between solution and crystalline states. Such observations have been made with other proteins (*19*). One way to explain our observation vis-à-vis X-ray crystallographic data is to assume a significant structural difference between the dimeric and monomeric forms of BoNT/A. X-ray crystallographic results are based on the monomeric form of BoNT/A (*6*) whereas spectroscopy-based secondary structure estimates were obtained at a BoNT/A concentration where it is expected to a dimer. Further experimental proof is needed to confirm this hypothesis.

Under reducing conditions, the secondary structure does not change significantly; however, the tertiary structure showed a significant difference between reduced and nonreduced toxin, as revealed by tryptophan fluorescence anisotropy spectra (Figure 2). Our observations suggest that the reduced toxin has a more flexible structure compared to the nonreduced toxin.

The crystal structure of BoNT/A (*6*) has revealed that the active site of BoNT/A is buried 20−24 Å deep within the protein matrix. The channel accessed to the active site is relatively small (~12 Å × 15 Å × 35 Å), and is partially shielded by the translocation domain of the toxin (*6*). This structural organization can be used to explain why reduction of the disulfide bond can help activate the endopeptidase activity of the toxin. We found that reduction of the disulfide bond increases the flexibility of toxin, a conclusion consistent with our earlier results (*7*). The flexible structure of the reduced toxin may make it easier for the 25 kDa SNAP-25 to access the enzyme's buried active site.

Analysis of the quaternary structure of BoNT/A in solution indicated that BoNT/A existed as a dimer in aqueous solution at high concentrations (above 75 nM) (Tables 1 and 2). This finding is in conflict with the recent X-ray crystallographic data, and suggests a different quaternary structural organization of BoNT/A in crystal and in solution. This is not abnormal, as quaternary structural differences between crystal and solution have been observed with other proteins (*19*). The observation we have made here is consistent with earlier findings from dynamic light scattering (*14*) and native gel electrophoresis (*12*), even though the latter report did not correct the charge interference in the native gel electrophoresis method.

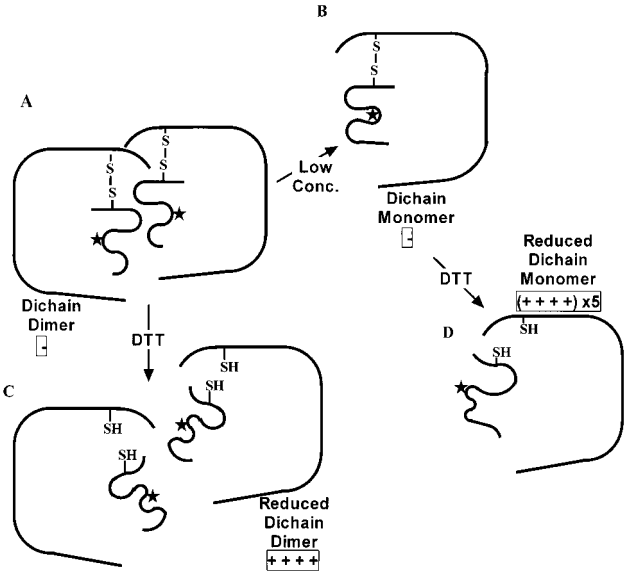

FIGURE 10: A working model of BoNT/A structure. Under nonreducing conditions, both dimeric (A) and monomeric (B) forms of the toxin do not show any enzymatic activity due to the buried active site. Under reducing conditions, the active site of the dimeric form of toxin gets partially exposed (C), exhibiting moderate enzymatic activity. The monomerization of reduced BoNT/A exposes the active site further (D), exhibiting a higher enzyme efficiency. The star represents the active site of the toxin. Negative (−) and positive (+) signs represent the absence and presence of enzyme activity.

The conclusion of a transition from the dimeric to the monomeric form of BoNT/A at a concentration of 50−75 nM suggests that BoNT/A exists in a monomeric form under physiological conditions. Both native and reduced forms of the toxin follow similar transition patterns between dimeric and monomeric forms. However, the estimated molecular sizes of reduced BoNT/A were significantly different (Table 2). This could be explained by assuming an alteration in the molecular shape of the protein, which will be consistent with our fluorescence anisotropy data (Figure 2), suggesting a more flexible structure of BoNT/A when its intersubunit disulfide bond is reduced.

The biological activity difference between dimeric and monomeric forms of BoNT/A (Table 3) indicates that the dimeric form of BoNT/A even under reducing conditions only partially opens its active site, whereas the active site is fully accessible in the monomeric form of BoNT/A under reducing conditions (Figure 10). This reveals a novel mechanism of activation of an endopeptidase. Inhibition of endopeptidase activity by disulfide-linked multimerization has been shown in the rat testicular endopeptidase EC 3.4.24.15 (*41*). Our observation here presents the first example where the enzymatic activity of an endopeptidase can be enhanced by self-dissociation of its oligomeric form into its monomeric form.

The physiological role of the quaternary structure of BoNT/A could also be related to its translocation into the nerve cell. As part of its mode of action, BoNT/A is known to form a membrane pore in endosomes at low pH. It has

been proposed that oligomeric species of BoNT/A are involved in pore formation (*10*, *42*). The observation of dimeric and monomeric species of BoNT/A in solution suggests a possible equilibrium between them, which could change under different pH conditions. It is possible that the oligomeric species of BoNTs are formed in the membrane to form the pore (*43*), while the pore is only large enough to translocate the monomeric form of BoNTs (or their light chains) into the neuronal cytosol (*44*). A physiological observation relevant to this suggestion is BoNT/A's differential effect on mouse phrenic diaphragm at different concentrations (*45*, *46*).

In summary, we have analyzed the structure of BoNT/A in aqueous solution using a comprehensive set of techniques for the first time. The structural organization at both the secondary and quaternary levels in aqueous solution is different from that reported for the crystalline state. The disulfide bond reduction does not change the secondary and quaternary structural organization of BoNT/A, but the shape of the dimeric structure of BoNT/A under reducing conditions is more flexible compared to that of the native toxin. The dimeric form of BoNT/A can be self-dissociated into the monomeric form at low concentrations. The enzymatic activity of the monomeric form of BoNT/A, on the other hand, is 4-fold higher than that of the dimeric form. These observations suggest a strong role of the BoNT/A quaternary structure in its molecular action against nerve endings, and may particularly suggest that the catalytic site of toxin is sterically restricted in the dimeric form.

Observations presented in this report will have significant impact on two biomedically critical aspects of botulinum neurotoxin research: (i) An understanding of the molecular structure of monomeric BoNT/A at physiological concentration will allow design of antidotes against botulism. (ii) The possibility of using a low dose of BoNT/A in clinical use will minimize immunogenic response in patients avoiding nonresponse after prolonged use (*47*).

REFERENCES

1. Montecucco, C., and Schiavo, G. (1995) *Q. Rev. Biophys. 28*, 423−472.
2. Krieglstein, K. G., Henschen, A. H., Weller, U., and Habermann, E. (1991) *Eur. J. Biochem. 202*, 41−51.
3. Dekleva, M. L., and DasGupta, B. R. (1989) *Biochem. Biophys. Res. Commun. 162*, 767−772.
4. Montecucco, C., Papini, E., and Schiavo, G. (1994) *Experientia 15*, 1026−1032.
5. Tonello, F., Morante, S., Rossetto, O., Schiavo, G., and Montecucco, C. (1996) in *Intracellualr protein catabolism* (Suzuki, K., and Bond, J., Eds.) pp 251−260, Plenum Press, New York.
6. Lacy, D. B., Tepp, W., Cohen, A. C., DasGupta, B. R., and Stevens, R. C. (1998) *Nat. Struct. Biol. 5*, 898−902.
7. Cai, S., Sarkar, H. K., and Singh, B. R. (1999) *Biochemistry 38*, 6903−6910.
8. Lebeda, F. J., and Olson, M. A. (1994) *Proteins: Struct., Funct., Genet. 20*, 293−300.
9. Singh, B. R., and DasGupta, B. R. (1989) *Mol. Cell. Biochem. 86*, 87−95.
10. Singh, B. R. (1996) in *Natural Toxins 2: Structure, Mechanism of Action, and Detection* (Singh, B. R., and Tu, A. T., Eds.) pp 63−84, Plenum, New York.
11. Shone, C. C., Hambleton, P., and Melling, J. (1985) *Eur. J. Biochem. 151*, 75−82.
12. Ledoux, D. N., Be, X. H., and Singh, B. R. (1994) *Toxicon 32*, 1095−1104.
13. Stevens, R. C., Evenson, M. L., Tepp, W., and DasGupta, B. R. (1991) *J. Mol. Biol. 222*, 877−880.
14. Stevens, R. C. (1993) in *Botulinum and tetanus neurotoxins* (DasGupta, B. R., Ed.) pp 393−395, Plenum Press, New York.
15. Cashikar, A. G., and Rao, N. M. (1996) *J. Biol. Chem. 271*, 4747−4746.
16. Philo, J. S., Rosenfeld, R., Arakawa, T., Wen, J., and Narhi, L. O. (1993) *Biochemistry 32*, 10812−10818.
17. Mei, G., Di Venere, A., Buganza, M., Vecchini, P., Rosato, N., and Finazzi-Agro, A. (1997) *Biochemistry 36*, 10917−10922.
18. Lubkowski, J., Bujacz, G., Boque, L., Domaille, D. J., Handel, T. M., and Wlodawer, A. (1997) *Nat. Struct. Biol. 4*, 64−69.
19. Singh, B. R., Fu, F.-N., and Ledoux, D. N. (1994) *Nat. Struct. Biol. 1*, 358−360.
20. Schiavo, G., Benfenati, F., Poulain, B., Rossetto, O., Polverinao de Laureto, P., DasGupta, B. R., and Montecucco, C. (1992) *Nature 359*, 832−835.
21. Blasi, J., Chapman, E. R., Link, E., Binz, T., Yamasaki, S., De Camilli, P., Sudhof, T. C., Niemann, H., and Jahn, R. (1993) *Nature 365*, 160−163.
22. Li, L., and Singh, B. R. (1999) *J. Toxicol., Toxin Rev. 18*, 95−112.
23. Montecucco, C., and Schiavo, G. (1993) *Trends Biochem. Sci. 18*, 324−327.
24. Ahnert-Hilger, G., and Bigalke, H. (1995) *Prog. Neurobiol. 46*, 83−96.
25. Schiavo, G., Rossetto, O., Tonello, F., and Montecucco, C. (1995) *Curr. Top. Microbiol. Immunol. 195*, 257−274.
26. Coffield, J. A., Bakry, N., Zhang, R.-D., Carlson, J., Gomella, L. G., and Simpson, L. L. (1997) *J. Pharmacol. Exp. Ther. 280*, 1489−1498.
27. Fu, F.-N., Sharma, S. K., and Singh, B. R. (1998) *J. Protein Chem. 17*, 53−60.
28. Hames, B. D., Ed. (1998) *Gel electrophoresis of proteins, a practical approach*, 3rd ed., pp 35−40, Oxford University Press, New York.
29. Chrambach, A., and Rodbard, D. (1971) *Science 172*, 440.
30. Rothe, G. M. (1991) *Adv. Electrophor. 4*, 251−358.
31. Molecular Probes Product Information (1999) Amine-reactive probes, Molecular Probes, Eugene, OR.
32. Lakowicz, J. R. (1983) *Principles of fluorescence spectroscopy*, pp 111−114, Plenum Press, New York.
33. Cai, S., and Singh, B. R. (1999) *Biophys. Chem. 80*, 7−20.
34. Retanal, C., and Babul, J. (1988) *Anal. Biochem. 175*, 544−547.
35. Culter, P. (1991) in *Protein purification protocols* (Doonan, S., Ed.) pp 255−268, Humana Press, Totowa, NJ.
36. Wong, S. S. (1991) *Chemistry of protein conjugation and cross-linking*, CRC Press, Boca Raton, FL.
37. Margosiak, S. A., Vanderpool, D. L., Sisson, W., Pinko, C., and Kan, C. (1996) *Biochemistry 35*, 5300−5307.
38. Fink, A. L. (1998) *Folding Des. 3*, R9−R21.
39. Herron J., and Voss, E. W., Jr. (1981) *J. Biochem. Biophys. Methods 5*, 1−17.
40. Schiavo, G., Santucci, A., DasGupta, B. R., Mehta, P. P., Jontes, J., Benfenati, F., Wilson, M. C., and Montecucco, C. (1993) *FEBS Lett. 335*, 99−103.
41. Shrimpton, C. N., Glucksman, M. J., Lew, R. A., Tullai, J. W., Margulies, E. H., Roberts, J. L., and Smith, A. I. (1997) *J. Biol. Chem. 272*, 17395−17399.
42. Singh, B. R., and Lebeda, F. (1999) *J. Toxicol., Toxin Rev. 18*, 45−76.
43. Schmid, M. F., Robinson, J. P., and DasGupta, B. R. (1993) *Nature 364*, 827−830.
44. Donovan, J. J., and Middlebrook, J. L. (1986) *Biochemistry 25*, 2872−2876.
45. Bandyopadhyay, S., Clark, A. W., DasGupta, B. R., and Sathyamoorthy, V. (1987) *J. Biol. Chem. 262*, 2660−2663.
46. Maisey, E. A., Wadsworth, J. D. F., Poulain, B., Shone, C. C., Melling, J., and Gibbs, P. (1988) *Eur. J. Biochem. 177*, 683−691.
47. Brin, M. E. (1997) *Muscle Nerve, Suppl. 6*, s146−s168.

BI0025363